Using Pseudopotentials within the Interacting Quantum Atoms Approach

Davide Tiana,‡ E. Francisco, M. A. Blanco, and A. Martín Pendás*

Departamento de Química Física y Analítica. Facultad de Química, Universidad de Oviedo, 33006-Oviedo, Spain

Received: February 25, 2009; Revised Manuscript Received: May 19, 2009

A general strategy to extend the interacting quantum atoms (IQA) approach to pseudopotential or effective core potential electronic structure calculations is presented. With the protocol proposed here, the scope of IQA thinking opens to chemical bonding problems in heavy-atom systems, as well as to larger molecules than those presently allowed by computational limitations. We show that, provided that interatomic surfaces are computed from core-reconstructed densities, reasonable results are obtained by integrating reduced density matrices built from the pseudowave functions. Comparison with all-electron results in a few test systems shows that exchange-correlation energies are better reproduced than Coulombic contributions, an effect which is traced to inadequate atomic populations and leakage of the core population into the surrounding quantum atoms.

Introduction

The interacting quantum atoms (IQA) approach[1–5] provides a fruitful theory of cohesion within the quantum theory of atoms in molecules (QTAIM) developed by Richard Bader and coworkers.[6] IQA is based on extending the characteristic QTAIM partitioning of one-electron observables into domain contributions to the two-electron components of the Hamiltonian, which now get decomposed into the sum of one- (or intra-atomic) or two-domain (or interatomic) terms. This introduces an exact, chemically appealing decomposition of the molecular energy into intra- and interatomic quantities (which we call self and interaction energies, respectively) with clear physical meaning and no external references. IQA interaction energies are directly composed of purely quantum mechanical and classical contributions. Hence, their classification using the chemical language of covalency and ionicity becomes natural.[4] The IQA approach is now in a relatively mature state and has been applied in several fields, such as to cast light on a number of interesting chemical bonding problems, ranging from the origin of the binding energies of simple diatomics[7] to the nature of hydrogen bonding,[8] to provide a real space view of some controverted issues like the origin of steric repulsions or simple rotation barriers,[9] or even to suggest a new general interpretation of the meaning of bond critical points as privileged exchange channels in molecules.[10] It has also been used to propose an interesting statistical interpretation of chemical bonds in terms of electron number distribution functions (EDFs).[11–14]

IQA analyses, necessarily based on numerical integration techniques, are computationally intensive, power scaling with the number of electrons, basis set functions, and (partially) occupied orbitals.[1] Moreover, small numerical errors when integrating the core regions of heavy atoms amplify themselves to large energetic uncertainties that may decrease the accuracy of the IQA interaction energies that is needed for chemical bonding problems. IQA has thus only been applied up to now to small molecular systems composed of light atoms, although it is clear that its use in larger molecules with heavier atoms would be highly desirable. This is particularly true in the case of transition-metal compounds, the natural home of a number of key concepts in the modern theory of the chemical bond. Among them, we may just cite the nature of formally multiple metal−metal bonds[15,16] or of agostic interactions[17] and concepts like back-donation,[18,19] the versatility of the metal−carbon bond,[20] and so forth. The use of QTAIM has also provided new interesting ideas in transition-metal chemistry, like that of ligand-induced charge concentrations (LICC).[21,22] Actually, transition-metal compounds have become one of the most active areas of application of the QTAIM theory in the last years.[23]

Most modern electronic structure calculations in heavy-atom molecules also struggle with the problem posed by the large number of chemically inert core electrons. This is almost invariably tackled by using either pseudopotentials (PP)[24] or, in general, effective core potentials (ECP's),[25] one-electron operators that act on valence electrons and prevent them from collapsing onto core states. If we wish to deal with heavy atoms in IQA, we have to face this de facto standard. The absence of cores would contribute to solve the numerical problems briefly described in the last paragraph. However, this very absence has also an obvious drawback within the QTAIM for the electron density $\rho(\boldsymbol{r})$ constructed from pseudovalence orbitals lacks the maxima (cusps, rigorously speaking) at the nuclear positions that define the atomic basins within the theory. This means that even though the PP energetics is well-behaved, the topology of the valence-only density, $\rho_{pp}(\boldsymbol{r})$, may be completely different from that obtained with the all-electron ρ. This difficulty is well-known in the literature, and several works[26,27] have been devoted to elucidate how to bypass it.

The aim of this paper is to examine different possibilities to perform IQA analyses on PP- (or ECP-) based wave functions. After assessing them, we will establish a simple protocol that opens a route to real-space descriptions of chemical bonds in transition-metal compounds. Our goal here is three-fold. First, we show how to solve the different technical issues posed by the absence of core electrons in the IQA integrations. Second, we examine how the PP-based IQA bonding quantities compare to actual all-electron (AE) results. For this comparison to be meaningful, we need accurate IQA results at the AE level.

* To whom correspondence should be addressed. E-mail: angel@fluor.quimica.uniovi.es.

‡ On leave from the Department of Structural Chemistry and Inorganic Stereochemistry, University of Milan, via Venezian 21, 20133 Milan, Italy.

10.1021/jp901753p CCC: $40.75
Published on Web 06/18/2009

Therefore, we have chosen a very simple set of test systems, CH_4, SiH_4, and GeH_4, for which AE and PP wave functions are easily constructed with several core sizes. Finally, we want to show how the protocol is used by commenting on a production run on GeH_4 from the bottom up. IQA descriptions of transition-metal compounds will be deferred for future publications.

The rest of the paper is organized as follows. First, we sketch the IQA approach in order to introduce the quantities that will be used in the rest of the paper. After this, a brief comment on how to obtain the correct topology of ρ from PP calculations, since this is a prior step to any IQA description, will be made. We will then first describe the problems associated with reconstructing full-electron IQA interactions from PP descriptions, our protocol in the cases of small and large cores, and the above-mentioned production run. We end the paper with a summary and some conclusions.

A Sketch of the IQA Approach

Starting from a QTAIM partitioning of the physical space, IQA[1–4] provides an exact, general decomposition of the total molecular energy into basin contributions (see refs 28 and 29 for an equivalent partition of the SCF energy, which is a particular case of the partition of the exact energy provided by us)

$$E = \sum_A \int_{\Omega_A} \mathrm{d}\boldsymbol{r}_1 \left(\hat{T} - \sum_B \frac{Z_B}{r_{1B}} \right) \rho(\boldsymbol{r}_1; \boldsymbol{r}'_1) + \frac{1}{2} \sum_{A,B} \int_{\Omega_A} \mathrm{d}\boldsymbol{r}_1 \int_{\Omega_B} \mathrm{d}\boldsymbol{r}_2 \frac{\rho_2(\boldsymbol{r}_1, \boldsymbol{r}_2)}{r_{12}} + \sum_{A>B} \frac{Z_A Z_B}{R_{AB}} \quad (1)$$

where Ω_A is the basin of nucleus A and ρ and ρ_2 are the first- and second-order spinless reduced density matrices, respectively. IQA uses chemical insight to gather the different energetic terms much in the light of McWeeny's[30] theory of electronic separability. This results in

$$E = \sum_A (T_A + V_{\mathrm{en}}^{AA} + V_{\mathrm{ee}}^{AA}) + \sum_{A>B} (V_{\mathrm{nn}}^{AB} + V_{\mathrm{en}}^{AB} + V_{\mathrm{ne}}^{AB} + V_{\mathrm{ee}}^{AB}) = \sum_A E_{\mathrm{self}}^A + \sum_{A>B} E_{\mathrm{int}}^{AB} \quad (2)$$

where the en, ne, ee, and nn subscripts refer to electron−nucleus, nucleus−electron, electron−electron, and nucleus−nucleus interactions between superscripted pairs of basins. Other QTAIM topological energy partitions have also been explored, particularly by Popelier et al.[31,32] All intrabasin terms are added to define a group's self energy, E_{self}^A, and all interbasin ones are added to construct the interaction energy between pairs of groups, E_{int}^{AB}. If binding energies with respect to given group's energetic references, $E_{\mathrm{self}}^{A,0}$, are needed, we also introduce group deformation energies

$$E_{\mathrm{def}}^A = E_{\mathrm{self}}^A - E_{\mathrm{self}}^{A,0} \quad (3)$$

Thus, binding in IQA comes from the balance between group deformation (or promotion, usually positive) and intergroup interaction (overall negative)

$$E_{\mathrm{bind}} = \sum_A E_{\mathrm{def}}^A + \sum_{A>B} E_{\mathrm{int}}^{AB} \quad (4)$$

Decomposing[2] ρ_2 into Coulombic and exchange-correlation contributions, $\rho_2 = \rho_2^{\mathrm{C}} + \rho_2^{\mathrm{xc}}$, with $\rho_2^{\mathrm{C}}(\boldsymbol{r}_1,\boldsymbol{r}_2) = \rho(\boldsymbol{r}_1)\rho(\boldsymbol{r}_2)$, each intergroup interaction may be divided into a classical, $V_{\mathrm{cl}}^{AB} = (V_{\mathrm{nn}}^{AB} + V_{\mathrm{en}}^{AB} + V_{\mathrm{en}}^{BA} + V_{\mathrm{C}}^{AB})$, and an exchange-correlation (nonclassical, quantum) term, V_{xc}^{AB}, so that

$$E_{\mathrm{int}}^{AB} = V_{\mathrm{cl}}^{AB} + V_{\mathrm{xc}}^{AB} \quad (5)$$

We have shown[3,5] that these two components are associated with the classical notions of ionicity and covalency; therefore, IQA provides a clean theoretical window to standard chemical thinking.

The Topology of ρ from Pseudopotential Calculations

As briefly explained in the Introduction, the absence of core electrons in PP or ECP electronic structure calculations poses some important problems in determining the topology of $\rho(\boldsymbol{r})$.[21,33] The key feature of valence-only densities is the lack of (3, −3) critical points (CPs) at the nuclear positions affected by core removal, which are sometimes substituted by (3, +3) CPs. Since the Poincaré-Hopf (or Morse) topological invariant must retain its value and the indices of (3, −3) and (3, +3) CPs are of opposite sign, the substitution of a maximum by a minimum must be necessarily accompanied by the creation of other compensating CPs, including at least either one maximum or one (3, +1) ring CP. As $\rho(\boldsymbol{r})$ is relatively unaffected at $\boldsymbol{r}$ points far enough from the removed cores, these new CPs are expected to lie in the vicinity of the latter, and the topology of ρ_{pp} is expected to resemble closely that of the AE density in the chemically relevant valence regions. Early explorations confirmed this in some cases[34] but not in others.[35]

A detailed analysis of these issues was performed by Vyboishchikov, Sierraalta, and Frenking.[27] These authors showed that correct topologies may be obtained from core-reconstructed pseudo-AE densities. Two different procedures were analyzed. In the first one, which we will label aug for augmented, the pseudo-AE density, ρ_{aug}, is found by adding a core density generated in an independent in vacuo atomic calculation, ρ_{core}, to the valence-only density, ρ_{ecp}, that is, $\rho_{\mathrm{aug}} = \rho_{\mathrm{ecp}} + \rho_{\mathrm{core}}$. In the second one, the core orbitals are orthogonalized to the valence ones, and the pseudo-AE density, ρ_{orth}, is derived from the orthogonalized determinant. Orthogonalized densities yielded no clear-cut improvement over either the local properties at critical points or the integrated ones over atomic basins. In fact, atomic populations and bond orders were shown to worsen considerably with respect to AE values, this effect being traced to the diffuse tails induced in the core orbitals upon orthogonalization.

We should also notice that the orthogonalization scheme is computationally equivalent (as CPU time is considered) to an IQA/AE calculation. Since our goal is both to decrease the computational effort of IQA integrations as well as to avoid numerical instabilities introduced by core electrons, we will not consider core orthogonalizations in the following. We should not forget, nevertheless, that sometimes the electronic structure optimization step, not the IQA computation, will be the computational bottleneck. In these cases, ECP pseudo-wave functions will always be preferred.

Table 1 reports the full topologies found for CH_4, SiH_4, and GeH_4. All of the electronic structure calculations have been

TABLE 1: Full Topologies of All-Electron (AE), Pseudo-Valence (ECP), and Core-Reconstructed (Aug) Densities for Methane, Silane, and Germane[a]

X (XH_4)	CP	position	$x(y)$	d	ρ	$\nabla^2\rho$	H
C(AE)	−1	(*x*,*x*,*x*)	0.7394	1.2807	0.2815	−1.0118	−0.2974
C(ECP)	+3	(0,0,0)		0.0000	9×10^{-5}	28.1304	−0.1295
	+1	(*x*,*x*,*x*)	0.3361	0.5821	0.2358	−0.7615	−0.8228
	−1	(0,0,*x*)	0.6177	0.6177	0.2547	−1.1119	−0.8196
	−3	(*x*,*x*,*x*)	0.4409	0.7637	0.2940	−1.4904	−0.6208
	−1	(*x*,*x*,*x*)	0.7243	1.2545	0.2797	−1.1088	−0.3005
C(aug)	−1	(*x*,*x*,*x*)	0.7266	1.2585	0.2798	−1.0006	−0.2986
Si(AE)	−1	(*x*,*x*,*x*)	0.7724	1.3378	0.1195	0.3018	−0.0711
Si(ECP)	−3	(0,0,0)		0.0000	5×10^{-8}	−0.8607	−0.2154
	+3	(*x*,*x*,*x*)	0.0273	0.0473	4×10^{-8}	0.0004	−0.0002
	+1	(*x*,*y*,*y*)	0.0319 (−0.0251)	0.0516	4×10^{-8}	0.0005	−0.0002
	+3	(0,0,*x*)	0.0550	0.0550	9×10^{-8}	0.0022	−0.0004
	+1	(*x*,*x*,*y*)	0.0186 (−0.0500)	0.0565	1×10^{-8}	0.0024	−0.0002
	+3	(*x*,*x*,*x*)	−0.0336	0.0582	7×10^{-8}	0.0027	−0.0004
	+1	(*x*,*x*,*x*)	−0.7526	1.3035	0.0338	−0.0251	−0.0228
	−1	(0,0,*x*)	1.3835	1.3835	0.0508	−0.0536	−0.0392
Si(aug)	−1	(*x*,*x*,*x*)	0.7957	1.3782	0.1222	0.1997	−0.0595
Ge(AE)	−1	(*x*,*x*,*x*)	0.9688	1.6780	0.1342	0.0581	−0.0878
Ge(ECPl)	−3	(0,0,0)		0.0000	1×10^{-6}	−1.0549	−0.2637
	+3	(*x*,*x*,*x*)	−0.0067	0.0116	1×10^{-10}	0.0083	−0.0000
	−3	(*x*,*x*,*x*)	0.0152	0.0263	2×10^{-7}	−0.0028	−0.0009
	−1	(*x*,*x*,*x*)	−0.0181	0.0314	2×10^{-7}	−0.0022	−0.0008
	+1	(*x*,*y*,*y*)	0.0018 (0.0250)	0.0354	1×10^{-7}	0.0246	−0.0004
	+3	(0,0,*x*)	0.0389	0.0389	8×10^{-10}	0.0056	−0.0000
	+1	(*x*,*x*,*x*)	−0.8174	1.4158	0.0368	−0.0453	−0.0302
	−1	(0,0,*x*)	1.4851	1.4851	0.0484	−0.0769	−0.0377
Ge(ECPs)	−3	(0,0,0)		0.0000	1×10^{-6}	−1.0497	−0.2624
	−1	(*x*,*y*,*y*)	0.1941 (0.0711)	0.2186	0.1329	0.0157	−0.0905
	+3	(0,0,*x*)	0.2836	0.2836	7.4371	−312.22	−356.29
	−3	(*x*,*x*,*x*)	−0.1638	0.2837	7.4680	−319.93	−357.22
	−3	(*x*,*x*,*x*)	0.1660	0.2875	0.3674	−21.539	−5.3861
	−1	(*x*,*x*,*x*)	0.9505	1.6463	0.1329	0.0151	−0.0905
Ge(augl)	−1	(*x*,*x*,*x*)	0.9825	1.7017	0.1364	0.0369	−0.0820
Ge(augs)	−1	(*x*,*x*,*x*)	0.9794	1.6964	0.1359	0.0389	−0.0849

[a] Molecular geometries are fixed at the AE-optimized values. All CPs are nondegenerate, classified according to their signatures with nuclear cusps ignored, and ordered according to their distance to the X nucleus, *d*. Only nonequivalent by symmetry CPs, together with their densities, laplacians, and energy densities, are reported. The multiplicities of CPs are 1, 4, 6, and 12 for the (0,0,0), (*x*,*x*,*x*), (*x*,0,0), and (*x*,*x*,*y*) special positions, respectively. All data are in au.

performed with the GAMESS[36] code at the Hartree−Fock level, using standard 6-311G(d,p) basis sets with CRENBL shape-consistent ECP's.[37,38] Changing the basis set, the ECP recipe, or the level of calculation does not alter significantly our conclusions, which are of a rather general validity. Two and ten electron cores have been used for C and Si, respectively, while both large (l, 28 e) and small (s, 18 e) cores are presented for Ge. In order to isolate the effect that the use of ECP's has on the topology from geometry optimization issues, all of the systems are studied at the AE-optimized geometries, and all topologies are found with our PROMOLDEN code. Although IQA allows for a correlated wave function, the simplicity of the Hartree−Fock model has been chosen to assess the best IQA/ECP strategy.

Let us comment on some interesting points. First, let us notice that all ECP topologies contain spurious CPs, whose number tends to increase with the size of the ECP core. Notice that in both the CH_4 and the small-core GeH_4 cases, we may define a confinement sphere, with radius r_s, completely contained within the AE central atom basin and containing all of the core CPs. A simple scan of Table 1 shows that in the CH_4 and GeH_4 molecules, $r_s \approx 0.77$ and 0.29 bohr, respectively. Notice that the core topologies in the two systems are different. In CH_4, the carbon nuclear cusp has been substituted by a cage CP, while a very small, though clearly developed, maximum is found in germane. The valence topology outside of the confinement sphere coincides with that in the AE calculation, although the quantitative details may differ. For instance, the position of the X−H bond critical points (bcps), together with their electron densities and energy densities, are recovered within 3% error. However, other more sensitive properties like $\nabla^2\rho$ are found to accumulate much larger errors. This behavior is typical of very compact cores.

The situation for the other cases is more complex. In both silane and germane, the confinement sphere cannot be defined since the AE valence topology is severely affected. No CP is found in the valence region along the bond directions. In fact, ρ grows monotonously from the X core toward the H maxima, and four (*x*,*x*,*x*) ring CPs appear in the rear bond directions at about the same distance from X as the AE bcps. Well-developed bcps appear between every pair of H's, in accord with the results of ref 27. A QTAIM partitioning based upon these ρ_{ecp} would fail by assigning completely unphysical basins to the quantum atoms. This behavior is usual for larger cores that clearly penetrate the valence and for highly charged quantum atoms, like Si in silane (see Table 2).

Addition of core densities, obtained by solving the ground-state electronic structure of the neutral isolated X atom with the same basis set used in the ECP calculation, recovers the AE topology in every case. The errors in ρ and H are less than 2 and 16%. However, although the errors in $\nabla^2\rho(r_{bcp})$ decrease upon adding core densities, they may be as large as 40%. Since

TABLE 2: IQA Decomposition for XH_4, X = C, Si, Ge[a]

X	Q(X)	E^{X}_{self}	E^{X}_{def}	E^{H}_{self}	V^{XH}_{cl}	V^{XH}_{xc}	δ^{XH}	V^{HH}_{cl}	V^{HH}_{xc}	δ^{HH}
C(AE)	0.1393	−37.4175	0.2668	−0.4396	0.0355	−0.2868	0.9825	0.0012	−0.0059	0.0432
C(pECP)	0.1390	−4.6298	0.1977	−0.4397	0.0355	−0.2867	0.9826	0.0012	−0.0059	0.0432
C(ECP)	0.1402	−5.4357	0.5128	−0.4390	0.0356	−0.2875	0.9823	0.0012	−0.0059	0.0433
C(aug)	0.1403	−37.9780	−0.2937	−0.4389	0.0356	−0.2876	0.9827	0.0012	−0.0059	0.0433
C(noxc)	0.1403	−37.8426	−0.1583	−0.4389	0.0354	−0.2875	0.9823	0.0012	−0.0059	0.0433
Si(AE)	2.9566	−286.6788	2.1666	−0.3273	−0.8916	−0.1150	0.4593	0.1440	−0.0167	0.1151
Si(pECP)	2.9286	0.2485	2.2918	−0.3676	−0.8703	−0.1101	0.4511	0.1409	−0.0166	0.1147
Si(ECP)	2.9292	−2.0304	2.2809	−0.3687	−0.8687	−0.1116	0.4501	0.1406	−0.0166	0.1152
Si(aug)	2.9538	−287.5160	1.3294	−0.3283	−0.8886	−0.1257	0.4873	0.1437	−0.0167	0.1155
Si(noxc)	2.9538	−287.3311	1.5143	−0.3273	−0.8886	−0.1167	0.4643	0.1437	−0.0166	0.1152
Ge(AE)	1.7977	−2074.3005	0.9715	−0.4251	−0.2745	−0.1884	0.7959	0.0434	−0.0062	0.0587
Ge(pECPl)	1.7230	1.6993	1.6604	−0.4752	−0.2469	−0.1766	0.7760	0.0394	−0.0063	0.0593
Ge(pECPs)	1.7949	−44.7902	1.0109	−0.4292	−0.2736	−0.1871	0.7949	0.0432	−0.0062	0.0587
Ge(ECPl)	1.7162	−3.1443	1.0427	−0.4718	−0.2464	−0.1789	0.7722	0.0393	−0.0063	0.0604
Ge(ECPs)	1.7570	−47.9161	0.9804	−0.4253	−0.2633	−0.1913	0.8016	0.0416	−0.0063	0.0603
Ge(augl)	1.7729	−2075.4851	−0.2131	−0.4244	−0.2678	−0.1965	0.8146	0.0424	−0.0062	0.0599
Ge(augs)	1.7598	−2075.4606	−0.1886	−0.4211	−0.2644	−0.1949	0.8114	0.0418	−0.0063	0.0603
Ge(noxcl)	1.7729	−2075.0803	0.1916	−0.4218	−0.2678	−0.1867	0.8007	0.0424	−0.0063	0.0604
Ge(noxcs)	1.7598	−2067.6789	7.5931	−0.4210	−0.2645	−0.1917	0.8030	0.0418	−0.0063	0.0603

[a] The all-electron results (AE) are to be compared with the three flavors of ECP and pseudo-ECP calculations (ECP, pECP, aug, and noxc) described in the text. All ECP and pECP wave functions have been obtained at the fixed AE geometries, and all interatomic surfaces are also frozen to those of the AE systems. The central atom deformation energies are measured with respect to ^{3}P in vacuo references. For the carbon atom, these are −37.6843, −4.8275, and −5.9485 au for the AE, pECP, and ECP calculations, respectively. For silicon, they are −288.8454, −2.0433, and −4.3113 au, respectively, and for germanium, they are −2075.2720, −45.8011,0.0389, −48.8965, and −4.1870 au in the AE, pECPs, pECPl, ECPs, and ECPl order. No deformation is given for H atoms, whose in vacuo self energy is constant to −0.4998 au. The computational conditions are shown in the text. All other data are also in au.

our goal is to compare integrated properties, a question remains, how do the rather big errors of high-order density derivatives near bcps in reconstructed densities translate into the final integrated data? From the purely topological point of view, the first requirement that we must meet is a faithful partition into atomic basins.

To test whether this is fulfilled by ρ_{aug} or not, we have examined not only the position of the CPs but the general structure of the interatomic surfaces (IAS) in a number of cases. For instance, Figure 1 shows this kind of analysis in GeH_4. The AE interatomic surfaces are rather faithfully reconstructed using ρ_{aug}, both in the small- and large-core cases. This is quite a general result that allows us to conclude that the usage of $\rho_{aug} = \rho_{ecp} + \rho_{core}$ provides an accurate enough framework to perform IQA integrations on ECP-based electronic structure calculations. Notice that when a confinement sphere may be defined, like in the GeH_4 ECPs model, the interatomic surfaces obtained from just ρ_{ecp} might also be trustful.

IQA Partitioning from ECP Pseudo-Wave Functions

Most modern ECP's or PPs are modeled as one-electron nonlocal operators acting on the valence electrons with the following algebraic structure[39]

$$V_{eff} = V_L(r) + \sum_{\lambda=0}^{L-1} \sum_{\mu=-\lambda}^{\lambda} |Y_{\lambda\mu}\rangle V_{\lambda-L}(r) \langle Y_{\lambda\mu}| \qquad (6)$$

$$V_{\lambda-L}(r) = V_\lambda(r) - V_L(r) \qquad (7)$$

In the above expressions, $L - 1$ is the maximum angular momentum of the excluded core electrons and the $l = \lambda - L$ dependent V's impose orthogonality constraints that avoid the collapse of the valence orbitals onto the core states. All of the spherical harmonics and radial functions are centered at the position of the atomic nucleus of the excluded core, and the $V_l(r)$ potentials are expressed as linear combinations of gaussians

$$V_l(r) = \sum_{i=1}^{N} B_i^l r^{n_i^l} \exp(-\alpha_i^l r^2) \qquad (8)$$

ECP pseudoenergies do not contain, manifestly, core self-energy contributions. Moreover, core−valence interactions are introduced in a mean-field manner through the effective one-electron potentials.

ECP descriptions are not strictly compatible with the first- and second-order density matrix partition provided by IQA. If we partition Tr ρV_{eff} in real space into basin contributions, the resultant atomic effective potentials, $V^A_{eff} = \int_{\Omega_A} d\mathbf{r} \mathrm{Tr}\, \rho V_{eff}$ will contain a mixture of effective one- and two-electron contributions. This violates the IQA spirit, in which every energetic quantity has both a clear physical meaning and a well-defined one- or two-electron nature. Much as the total expectation value of V_{eff} plays no role in ECP calculations, we deem that no chemical meaning should be assigned to the atomic V^A_{eff}'s. Thus, we do not consider them in our protocol.

Taking into account these constraints, together with the results of the previous section, we have devised three computational strategies. They all start by using an ECP pseudowave function to determine the interatomic surfaces (i.e., the atomic basins) of ρ_{aug}, obtained by adding the core densities ρ_{core} of all of the ECP atoms to ρ_{ecp}, as described before.

In the first strategy, IQA integrations are performed on first- and second-order density matrices, ρ_{ecp} and $\rho_{2,ecp}$, derived from the pseudovalence wave function Ψ and completely ignoring the energetic role of core electrons, which are, in a way, collapsed onto their corresponding nuclei. From a practical point of view, the nuclear charge of each ECP atom is decreased by the number of core electrons, $Z^A_{eff} = Z_A - n^A_{core}$, and a normal IQA calculation is performed afterward. These IQA-ECP (or

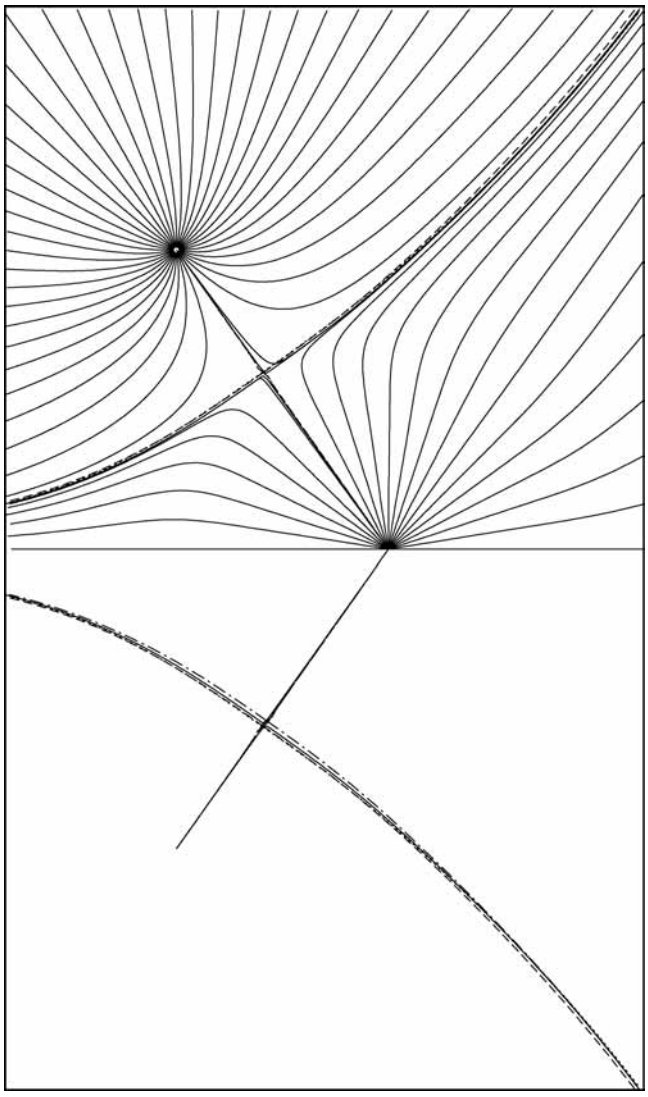

Figure 1. Comparison of the gradient field, including interatomic surfaces, of AE and core-reconstructed densities for GeH_4 in a plane containing a GeH_2 group. Full lines are used for AE results, and dotted and dashed−dotted lines are for large- and small-core data, respectively. Inner bulk gradient lines are only shown for the AE wave function in the upper part of the figure, so that the differences among the interatomic surfaces and bond paths are better appreciated in the lower symmetrical region, where we have also plotted (dot−dashed) the interatomic surface and bond path for the gradient field of ρ_{ecp} in the ECPs case.

simply ECP) results scale with a power of the number of valence electrons, n_{val}, which constitutes our goal.

A second possibility is to obtain pseudo-all-electron first- and second-order matrices constructed by augmenting with suitable core orbitals the pseudovalence. The cleanest procedure to do this, mutually orthogonalizing the chosen core orbitals to the pseudo-valence ones, leads to the errors commented on in the last section and has to be abandoned. Neglecting the orthogonality requirements, we arrive at $\rho_{aug} = \rho_{ecp} + \rho_{core}$. Since $\rho_{2,aug}$ can be written as $\rho_{2,aug} = \rho^{C}_{2,aug} + \rho^{xc}_{2,aug}$, where $\rho^{C}_{2,aug} = \rho_{aug}(\boldsymbol{r}_1)\rho_{aug}(\boldsymbol{r}_2)$ and $\rho^{xc}_{2,aug} = \rho^{xc}_{2,ecp-ecp} + \rho^{xc}_{2,core-core} + \rho^{xc}_{2,ecp-core}$, this approach (called IQA-aug, or simply aug) includes valence−valence, core−core, and core−valence interactions and is computationally equivalent to an AE IQA calculation. In this approach, an intrinsic error is introduced by using supposing orthogonality of a set of orbitals that is not rigorously orthogonal. As we will see, it is the core−valence exchange-correlation terms obtained with this scheme, coming from $\rho^{xc}_{2,ecp-core}$, that may be untrustworthy, a problem that may be traced back to the lack of both self-consistency and orthogonality between the core and the valence orbitals. For this reason, a third, mixed strategy has been used in which all core−valence exchange-correlation matrix elements are neglected, that is, $\rho^{xc}_{2,ecp-core} = 0$. With this, the core−valence interaction is reduced to its purely Coulombic terms, contained in the separated first-order core, ρ_{core}, and valence, ρ_{ecp}, densities. All core−core and valence−valence terms are explicitly included. We will call this procedure IQA-noxc, or simply noxc. Both the aug and noxc procedures allow us to perform IQA calculations from external ECP wave functions. However, we would like to stress that no significant computational saving is achieved with respect to an AE computation. Finally, we have also constructed pseudo-ECP (pECP) wave functions by deleting the appropriate core orbitals from the AE calculations. Densities ρ_{pecp} and $\rho_{2,pecp}$ are obtained as in the ECP procedure. IQA results on these pECP systems (IQA-pECP, or simply pECP in the following) will allow us to isolate core-removal effects from genuine alterations due to the ECP approximation.

Another point needs be clarified. Since, at this moment, we are mainly interested in isolating the errors introduced in the determination of the surfaces from those inherent to the IQA integration procedure, we will use the basins of the AE wave functions to obtain both AE IQA results and those of the three strategies just presented. This is easy to do with our PROMOLDEN code since the interatomic surfaces at fixed molecular geometry may be directly transported across systems described with different wave functions. This restriction will be freed in our production example.

Representative results are contained in Table 2. IQA integrations have been performed to $l_{max} = 10$, with 512 point radial and 3810 point Lebedev angular grids. β-spheres up to $l = 6$ with radii equal to 90% of the distance from the nuclear position to the closest bcp have been used, and 256 radial and 302 Lebedev angular grid points have been selected for them. These are fairly standard computational conditions for IQA calculations,[3] which ensure interactions converged to about 1 kcal/mol.

CH_4. Let us first examine the methane results with a very compact $1s^2$ ECP core. Any of our three ECP methodologies leads to a rather converged carbon basin net charge of 0.140 |e|, almost 0.001 e above the AE result. Under the assumption that the valence density is perfectly reconstructed by the ECP procedure, the difference in atomic populations (with frozen interatomic surfaces) between ECP and AE results should only come from core densities spreading over other interatomic basins, that is, from imperfect core localization. This spreading will be called core leakage and necessarily leads to X net charges less positive in ECP calculations. As seen in the table, this is the case in the pECP result but not in our ECP data for CH_4. Let us emphasize that even if core leakage may sound odd at first, it is clearly necessary for core densities extend, in principle, into the spatial regions occupied by the other quantum atoms. The core leakage in CH_4 may be easily obtained by integrating the core density in the C basin, turning out to be smaller than 0.1 me. With this, the me discrepancy has to be interpreted as a genuine small difference between the all-electron and effective core potential descriptions. To our accuracy, the C core is perfectly localized within its basin.

Turning to the CH_4 energetic contributions, all intrabasin terms have been gathered into atomic self and deformation energies in Table 2. Deformations have been computed with respect to in vacuo calculations at the Hartree−Fock (HF) level

in the ^{3}P state, as provided by GAMESS. Notice that exclusion of the core has a huge impact in E^{C}_{self}, as expected.

As E_{self}'s are regarded, even different AE basis sets for the same atom may yield differences in the au scale since the largest part of an atom's energy lies in the core regions. These differences amplify if ECPs are used, and E_{self} of the AE and ECP carbon atoms are about −37.4 and −5.4 au, respectively. Even the smallest distortion of the core regions has a huge impact on E_{self}'s. As another example, just changing the ECP orbitals by the frozen AE ones (the pECP model) modifies the carbon self energy by almost 0.8 au However, subtracting the free atoms' E^{A}_{self} to give E^{A}_{def} brings the latter discrepancies into a common (albeit large) scale.

If we further decompose the deformation energies into their components, $E_{def} = T^{def} + V^{def}_{ne} + V^{def}_{ee}$, we get for the C atom $T^{def} = 0.6499$, 0.1147, and −0.0232, $V^{def}_{ne} = -1.0316$, −0.8204, and −1.0801, and $V^{def}_{ee} = 0.8945$, 0.9034, and 1.3707 au, in the ECP, pECP, and AE order. Notice how the potential contributions tend to cancel. These data, together with the total $\Delta E_{def} \approx -0.25$ au between the ECP and AE results, show us that large energetic discrepancies (especially kinetic ones) exist between the core regions of the ECP pseudovalence and the AE valence orbitals. This means that, in the absence of V_{eff} contributions, no reliable binding energies may be obtained from IQA/ECP calculations. Chemically relevant interactions, depending on the valence, may however be safely obtained, as we are going to show. We will thus confirm by our treatment that chemistry is in the valence, although binding cannot be recovered without the cores, a very old idea put anew in real space.

Reconstruction of the core, either in the aug or noxc flavor, introduces new spurious errors in E^{C}_{self}, which come from (i) the lack of self-consistency between the atomic-based cores and the valence molecular orbitals and (ii) the nonorthogonality between core and valence states. As a result, the atomic C core is markedly less compact than the molecular one, and its E_{self} is artificially stable. The self energy of the H atom is seen to be barely affected by the presence/absence of the C core. This is a particularly desirable result that we want to emphasize. It requires that both the first-order (nondiagonal) and second-order density matrices be negligibly modified in the H basin by the C core, that is, that no core leakage and core delocalization within the H basin exist. The C core is thus chemically inert in real space from the self energy point of view, as expected.

If the C core is chemically inert as interactions are regarded, the HH quantities should be rather insensitive to its presence or absence. This is indeed found, and all of the HH energetic components plus δ^{HH} are converged at the ECP level. At any level of description, the HH delocalization provides a small, −3.7 kcal/mol, covalent stabilization between the H atoms, which decreases to about −2.9 kcal/mol when their small classical repulsion is taken into account. In principle, the CH interaction might feel the presence of even a completely localized core with no leakage through Coulombic effects beyond point charge interactions. This is not the case, and save a small systematic error in V^{XH}_{xc}, all CH quantities are basically converged in any of the three ECP computational schemes. We may thus conclude that the C core in methane behaves as an almost perfectly spherical distribution of electrons which are well localized in the C basin, both in the one- and two-electron sense. Its electrons may be collapsed onto the nucleus without chemically relevant consequences.

SiH_4. As silane is regarded, its large 10 e core is the clear counterpart of the compact C core just discussed. As core leakage is concerned, Table 2 shows that about 27 me of the core are finally contained in the H basins. Since, as a rule of thumb, electronic transfers (in e) are associated with equivalent energy changes (in au), this effect should be accompanied by sizable IQA energetic effects. We should first notice that the effect of cores on E^{Si}_{self} is now very large. Again, even if the ECP results show very similar interactions to those found at the pECP level, the behavior of the pseudovalence orbitals in the vicinity of the Si nucleus is quite different from that of the AE valence functions, and the pECP and ECP self energies of silicon differ by almost 1.8 au, although the AE, pECP, and ECP deformations are more transferable than those in methane. Now, the core-reconstructed self energies differ from the AE value by almost 1 Hartree. The effect on E^{H}_{self} is much smaller but not negligible. The ECP-only value differs by 26 kcal/mol from the AE one, although inclusion of the core, particularly at the noxc level, allows us to recover the AE results.

It is interesting to notice that HH interactions hold a key to interpret the above results since both E^{HH}_{xc} and δ^{HH} are converged even at the ECP level. Core leakage is thus a one-particle effect as the H atoms are concerned, and core electrons do not significantly participate in exchange interactions between two H atoms. The difference between HH interactions at the AE and ECP levels are thus due to the Coulombic effects of leakage. This is corroborated by our data. ECP-only IQA values, with no core electrons leaking into the H basins, provide decreased Coulombic repulsions between the H atoms in XH_4 compounds, especially for large-core ECP's. These anomalously small repulsions are partially restored upon reconstructing the cores by either of our two procedures.

The situation is different for the SiH pairs. Core leakage leads to quite larger Coulombic attraction between the Si and H atoms at the AE level than that at the ECP one. Once again, this effect is corrected by any of our aug or noxc strategies. However, contrarily to the HH case, a small exchange-correlation correction is also needed for the ECP V^{SiH}_{xc} is in error by 2 kcal/mol. The extra V^{SiH}_{xc} contribution introduced by the aug procedure spuriously overcorrects the SiH exchange-correlation interaction, inducing larger SiH delocalizations than those present at the AE level. In fact, the aug V^{SiH}_{xc} error is almost 7 kcal/mol. We think that this is due to the lack of self-consistency between the core and valence orbitals (including orthogonality). The noxc data, in which core−valence exchange is not allowed, corrects for this behavior.

Summarizing, the large Si core has a leakage of about 0.03 e into the H basins. Its effect is concentrated on the one-particle properties, and assuming that no two-basin delocalization occurs with these electrons is rather safe. The covalent contributions to the interactions are rather well reproduced at the ECP-only level, but the Coulombic ones will be in error to about the core leakage expressed in energetic au, about 15 kcal/mol. This is not a large quantity ($V^{SiH}_{cl} = -559$ kcal/mol) but needs be taken into account. Core reconstruction is preferred at the noxc level, but we should not forget that in doing so, we loose an important part of the computational saving of ECP pseudo-wave functions. As the pseudopotential or ECP approximations themselves are regarded, the comparison of AE and pECP results, on the one hand, and of pECP and ECP data, on the other, shows that the ECP method provides pseudovalence orbitals which reproduce rather well the AE distribution in the valence region but not in the vicinity of the nucleus.

GeH_4. Germane gives us the opportunity to examine all of the above effects in the 28 electron large-core (l) and 18 electron small-core (s) cases. First, core leakages are considerably larger

than those in the previous cases since the outer electrons in the He, Ne, and Ar closed shell series are less and less compact. Notice that the large core leaks about 0.8 e into the ligands and that this number is only halved by using the small [Ne] core. In other words, the 10 3d electrons leak out about as much charge as the [Ar] core. This is in agreement with common wisdom, and the 3d subshell has a similar extension as the 3s and 3p ones. The effect of the ECP approximation is non-negligible in the small-core case, and the Ge ECP pseudovalence orbitals have about 0.04 extra electrons in the core region as compared with the AE valence ones.

The germanium self or deformation energies follow the same patterns already encountered for carbon or silicon, and the small core leads to a deformation energy quite similar to that found at the AE level. Core reconstruction leads to very large deformation errors, particularly in the bs case. On the other hand, the E^{H}_{self} ECPl value is almost 30 kcal/mol larger than the AE one, but this error becomes very small for the ECPs case. Core reconstruction reduces considerably the error for the large core, particularly for the al case, and leads to a converged value (within 1 kcal/mol) in the as, bl, and bs approximations, still 2−3 kcal/mol above the AE value. Residual irreducible effects are thus larger in germane than those in our previous examples. For instance, any of our flavors leads to a consistent δ^{HH} value which is almost 0.002 units larger than the AE one. Its constancy points again to very slight interhydrogen delocalization of core electrons, though the discrepancy has to be interpreted as a genuine ECP effect.

The covalent contribution for the HH interaction, −3.9 kcal/mol, is almost one-third that in silane and similar to that found in methane. It is already well simulated by ECP-only results. Coulomb effects are, as usual, larger. V^{HH}_{cl} differs in the large ECP calculation by 2.6 kcal/mol from the AE result but only by 1.1 kcal/mol if the small core is used. If we examine the GeH pairs, a similar image arises. The δ^{GeH} is too low in the ECPl description, while it is reasonable in the ECPs one. The errors in the V^{SiH}_{xc} contribution are +6.0 and −1.8 kcal/mol, respectively. The greater core leakages now induce larger deviations of V^{GeH}_{cl} from the AE value, −17.6 and −10.6 kcal/mol for ECPl and ECPs, respectively.

Core reconstruction leads to an improvement of the GeH interaction terms, although an error of about 7 kcal/mol remains in the classical contribution. This clearly points toward a mixture of core polarization, orthogonality, and self-consistency effects affecting the one-particle charge distribution of the core. It is important to recognize at this moment that core reconstruction has a rather small energetic impact in the small-core case but a considerable one as the computational cost is regarded, if core−core electron repulsions are computed. For instance, the CPU time of any of the aug or noxc schemes for germane is about 13000 s in a 3.4 GHz 32 bit single processor machine, but this time decreases to 4800 and 1800 s in the ECPs and ECPl cases, respectively. We think that the balance between accuracy and computational cost should be selected depending on the particular needs of the study that is being undertaken.

A Production Example

As we have shown in the previous sections, reasonably accurate results may be obtained by performing IQA integrations on pseudovalence densities. Moreover, in terms of energetic accuracy versus computational cost, reconstruction of the core is really not necessary to account for chemical bonding issues, although the topology of the electron density, that is, the interatomic surfaces defining the integration domains, has to be obtained from a suitable core-reconstructed density.

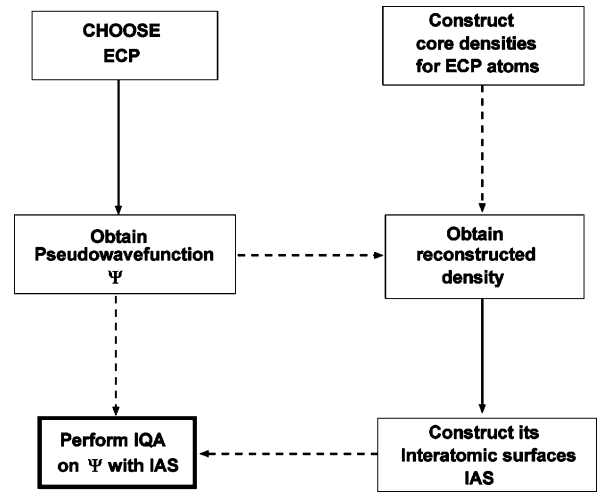

Figure 2. Scheme of our proposed protocol for IQA/ECP calculations. Full lines imply a direct connection between steps. Dashed lines stand for steps that need be fed with several inputs. For instance, to obtain the reconstructed density, we need both the core densities for ECP atoms and the pseudo-wave function from the chosen ECP model.

Our proposed protocol has five simple steps, (i) select the ECP description of the molecular system; (ii) obtain the pseudovalence description from any standard electronic structure code; (iii) construct adequate core densities for all atoms described by ECP's; a simple option for this is to perform in vacuo atomic calculations with the same basis sets used in the molecular case, but others exist; (iv) construct the interatomic surfaces of the reconstructed density, $\rho_{aug} = \rho_{core} + \rho_{ecp}$; and (v) integrate over the ρ_{aug} basins using first- and second-order density matrices obtained from the pseudo-wave function only, that is, our ECP strategy of the previous section. A scheme of this procedure is found in Figure 2.

Let us take germane as our production example. Optimization of geometries at the ECP level leads to differences inherent to the pseudopotential approximation. Table 3 has a summary of geometric and force constant data. Both small- and large-core ECP's induce a significant contraction of the Ge−H distance, although the harmonic frequencies are not much affected. This may be due to the use of nonrelativistic ECPs since it is known that better geometries are obtained with the latter.[40]

From the real-space point of view, this Ge−H distance shortening with no particular force constant change is associated with a redistribution of charge without much variation in the exchange-correlation contributions. Force constants depend much more abruptly on changes on V_{xc} than on those on V_{cl}. Table 4 has a summary of IQA data for both the large- and small-core calculations, to be compared with the corresponding ECPl/ECPs and AE lines in Table 2. The Ge atom is noticeably less charged in the optimized ECPs geometry than that in the one corresponding to the AE calculation. This is relatively easy to rationalize. Since the Ge cores clearly leak into the valence, their absence, even with the projection operators that preclude collapse of the valence orbitals onto core states, induces an artificial lack of core pressure on the valence electrons, and the Ge−H distance decreases. The effect of this decrease is clearly more important on the large-core situation. The use of relativistic cores may prevent these effects.

As we can see, the reduced net charge in Ge gives rise to smaller classical stabilization for the GeH pair. This is classical reasoning based on Coulomb's law for the change in geometry does not compensate for the larger change in charge transfer, the reduction being thus more important for the ECPl case. Small

TABLE 3: Ge−H Distance (in Å) and Harmonic Vibrational Frequencies (in cm^{-1}) Calculated for GeH_4 at the AE, ECPl, and ECPs Respective Optimum Geometries

	d(Ge−H)	ν_1	ν_2	ν_3	ν_4
AE	1.5315	912.3	993.3	2229.9	2255.7
ECPl	1.5170	934.8	1015.5	2214.4	2250.3
ECPs	1.5174	917.9	1009.0	2249.9	2273.5

TABLE 4: IQA Decomposition for Germane According to Our Proposed ECP Protocol[a]

	Q(Ge)	E_{self}^{Ge}	E_{def}^{Ge}	E_{self}^{H}	V_{cl}^{GeH}	V_{xc}^{GeH}	δ^{GeH}	V_{cl}^{HH}	V_{xc}^{HH}	δ^{HH}
ECPl	1.6898	−3.1680	1.0190	−0.4734	−0.2351	−0.1817	0.7784	0.0378	−0.0063	0.0598
ECPs	1.7104	−47.9542	0.9423	−0.4306	−0.2457	−0.1944	0.8107	0.0390	−0.0061	0.0587

[a] Computational conditions identical to those in Table 2. All data in au.

perturbations in charge transfers are usually accompanied by similar, though opposite, changes in E_{xc}. In our case, the absolute value of E_{xc}^{GeH} increases with respect to Table 2, and the ECPl and ECPs results bracket the AE energy. This is correlated with the equivalent bracketing in the GeH stretching frequencies shown in Table 3.

Flexion or bending modes are more related to the HH interactions, which are now dominated by the Coulombic terms. Now, they are consistently larger in the ECP calculations than in the AE one, corresponding to the smaller classical repulsions between the H atoms, particularly in the ECPl case.

Overall, the IQA/ECP description of germane gives rise to reasonably accurate covalent contributions for both the GeH and the HH pairs and introduces a charge-transfer bias related both to the too short Ge−H optimized distance and to the core leakage that we have already discussed in this work. Fortunately, this effect may be clearly anticipated from the failure of the ECP's used to provide an accurate geometry.

The amount of charge that leaks from the core of an atom A may be bounded from above if one computes the number of electrons lying within a sphere with a radius equal to the average of the distances from the nucleus A to all of its associated bcps. Since the atomic cores will be spherical almost always, this is a very easy task. These radii are equal to 0.678, 0.708, and 0.888 Å for the AE-optimized geometries of CH_4, SiH_4, and GeH_4, and the number of electrons of the core escaping their related spheres turns out to be 0.3, 86.9, 257.5, and 17.9 me, for the C, Si, Ge(l), and Ge(s) cores, respectively. We may indeed check that these are upper bounds to the actual core leakages. Another estimation of the errors coming from incorrect charge transfer in the IQA/ECP Coulombic terms may be obtained by looking at the differences in standard population analyses as provided by the electronic structure codes. We have found that Löwdin symmetrical populations reflect the trends in QTAIM changes more faithfully than Mulliken charges. For instance, the Löwdin Ge charges are 0.106, 0.080, and 0.086 |e| in the AE, ECPl, and ECPs descriptions at the AE-optimized geometries. The Mulliken ones are 0.477, 0.474, and 0.461, in the same order. In SiH_4, the equivalent Löwdin (Mulliken) AE and ECP charges are 0.522 (0.754), and 0.531 (0.771), respectively, and they are −0.240 (−0.359), and −0.239 (−0.325) in methane. Real-space partitioning amplifies these effects, but Löwdin populations provide a gross approximation to the expected IQA/ECP errors.

Summary and Conclusions

We have shown in this paper how the interacting quantum atoms approach[1–5] may be used with pseudovalence wave functions constructed under the pseudopotential or effective core potential approximations.

A few previous works[21,26,27,33] had already shown that the topology of ρ as directly determined from valence-only densities always contains a number of spurious critical points in the core regions. What is more important, depending on the size of the excluded core, the topology of the valence region, which defines the interatomic surfaces of the QTAIM approach, may be completely wrong. We have shown in a few examples that this is clearly true and that it is absolutely necessary to add a sensible core density to the pseudovalence one in order to recover reasonable topologies from ECP calculations. Our final recipe obtains core densities for the appropriate atoms and adds them to the valence pseudodensities. These core densities may, for instance, be obtained from in vacuo calculations in the isolated atoms. The pseudo all-electron densities are then used to obtain the interatomic surfaces defining the atomic basins.

In order to perform an IQA/ECP calculation once the interatomic surfaces have been constructed, we have examined three strategies. In the first one, the IQA/ECP protocol, all IQA quantities are obtained with reduced density matrices built from the pseudo-wave functions. This is our final goal, which exploits the ECP reduced number of electrons from a computational point of view. For comparison purposes, we have also devised two other strategies. The first (aug) uses an all-electron pseudo-wave function which comprises the core and the valence orbitals. This is a crude procedure since core orbitals are not self-consistent with the valence ones, this effect including nonorthogonality issues. The second (noxc) uses the (aug) approach but neglects all exchange-correlation terms between the core and the valence orbitals, which may be in large error due to the above-mentioned lack of self-consistency and/or orthogonality. We have also used pseudo-ECP descriptions by deleting core orbitals from AE calculations. In no case has the expectation value of the effective potential induced by the excluded core electrons been partitioned in real space since no clear physical meaning can be assigned to its atomic partition. Upon doing so, we would violate the IQA spirit.

Our results in the CH_4, SiH_4, and GeH_4 series, for which IQA AE data may also be obtained, show that ECPs rather faithfully reconstructs the valence regions of the AE valence orbitals, failing to do so in the vicinity of the nucleus. Large cores leak charge into the surrounding quantum atoms. This is mainly a one-electron effect, and the covalent contributions to IQA interactions are rather well approximated by the three procedures. Incorrect atomic populations may lead, however, to sizable errors in the classical contributions to the interactions. The magnitude of these errors may be grossly estimated by two methods. Inclusion of cores at either the aug or noxc level improves the agreement with the AE calculations, particularly as regards the classical terms. However, these two last approaches are computationally equivalent to all-electron IQA

calculations, and surpassing this computational bottleneck is one of the goals of the full IQA/ECP enterprise.

Fortunately, as, many times, we are interested in the IQA nonclassical (i.e., covalent) contributions to bonding, we think that conclusions drawn from the IQA/ECP simple protocol should be reliable in general, opening the way to IQA thinking in transition-metal chemistry. Further studies are under way.

Acknowledgment. D.T. thanks the University of Milan and the Italian Ministry of Research (MIUR) for a Ph.D. grant that allows his stay at Oviedo. We also acknowledge financial support from the Spanish MICINN, Project No. CTQ2006-02976, the European Union FEDER funds, and the MALTA-Consolider program (CSD2007-00045).

References and Notes

(1) Martín Pendás, A.; Blanco, M. A.; Francisco, E. *J. Chem. Phys.* **2004**, *120*, 4581.
(2) Martín Pendás, A.; Francisco, E.; Blanco, M. A. *J. Comput. Chem.* **2004**, *26*, 344.
(3) Blanco, M. A.; Martín Pendás, A.; Francisco, E. *J. Chem. Theory Comput.* **2005**, *1*, 1096.
(4) Francisco, E.; Martín Pendás, A.; Blanco, M. A. *J. Chem. Theory Comput.* **2006**, *2*, 90.
(5) Martín Pendás, A.; Blanco, M. A.; Francisco, E. *J. Comput. Chem.* **2007**, *28*, 161.
(6) Bader, R. F. W. *Atoms in Molecules*; Oxford University Press: Oxford, U.K., 1990.
(7) Martín Pendás, A.; Francisco, E.; Blanco, M. A. *J. Phys. Chem. A* **2006**, *110*, 12864.
(8) Martín Pendás, A.; Blanco, M. A.; Francisco, E. *J. Chem. Phys.* **2006**, *125*, 184112.
(9) Martín Pendás, A.; Blanco, M. A.; Francisco, E. *J. Comput. Chem.* **2009**, *30*, 98–109.
(10) Martín Pendás, A.; Francisco, E.; Blanco, M. A.; Gatti, C. *Chem. Eur. J.* **2007**, *13*, 9362.
(11) Francisco, E.; Martín Pendás, A.; Blanco, M. A. *J. Chem. Phys.* **2007**, *126*, 094102.
(12) Martín Pendás, A.; Francisco, E.; Blanco, M. A. *J. Phys. Chem. A* **2007**, *111*, 1084.
(13) Martín Pendás, A.; Francisco, E.; Blanco, M. A. *J. Chem. Phys.* **2007**, *127*, 144103.
(14) Martín Pendás, A.; Francisco, E.; Blanco, M. A. *Phys. Chem. Chem. Phys.* **2007**, *9*, 1087.
(15) Frenking, G. *Science* **2005**, *310*, 796.
(16) Gagliardi, L.; Pyykkö, P.; Roos, B. *Phys. Chem. Chem. Phys.* **2005**, *7*, 2415.
(17) Brookhart, M.; Green, M. L. H. *J. Organomet. Chem.* **1983**, *500*, 127.
(18) Dewar, M. *Bull. Soc. Chim. Fr.* **1951**, *18*, C79.
(19) Chatt, J.; Duncanson, L. A. *J. Chem. Soc.* **1953**, 2939.
(20) Weinhold, F.; Landis, C. *Valency and Bonding. A Natural Bond Orbital Donor−Acceptor Perspective*; Cambridge Univ. Press.: New York, 2005.
(21) Bader, R. F. W.; Gillespie, R. J.; Martín, F. *Chem. Phys. Lett.* **1988**, *290*, 488.
(22) Scherer, W.; McGrady, G. S. *Angew. Chem., Int. Ed.* **2004**, *43*, 1782.
(23) Macchi, P.; Sironi, A. *Coord. Chem. Rev.* **2003**, *238−239*, 383.
(24) Phillips, J. C.; Kleinman, L. *Phys. Rev.* **1959**, *116*, 287.
(25) Huzinaga, S.; Cantu, A. A. *J. Chem. Phys.* **1971**, *55*, 5543.
(26) Cioslowski, J.; Piskorz, P. *Chem. Phys. Lett.* **1996**, *255*, 315.
(27) Vyboishchikov, S. F.; Sierraalta, A.; Frenking, G. *J. Comput. Chem.* **1996**, *18*, 416.
(28) Mayer, I.; Hamza, A. *Theor. Chem. Acc.* **2001**, *105*, 360.
(29) Salvador, P.; Duran, M.; Mayer, I. *J. Chem. Phys.* **2001**, *115*, 1153–57.
(30) McWeeny, R. *Methods of Molecular Quantum Mechanics*, 2nd ed.; Academic Press: London, 1992; Chapter 14.
(31) Rafat, M.; Popelier, P. L. A. *J. Comput. Chem.* **2007**, *28*, 292.
(32) Darley, M. G.; Popelier, P. L. A. *J. Phys. Chem. A* **2008**, *112*, 12954.
(33) HÔ, M.; Schmider, H.; Edgecombe, K.; Smith, V. H. *Int. J. Quantum Chem.* **1994**, *52*, S215.
(34) Bo, C.; Poblet, J. M.; Bènard, M. *Chem. Phys. Lett.* **1990**, *141*, 380.
(35) Sierraalta, A.; Ruete, F. *J. Comput. Chem.* **1994**, *15*, 313.
(36) Schmidt, M. W.; Baldridge, K. K.; Boatz, J. A.; Elbert, S. T.; Gordon, M. S.; Jensen, J. H.; Koseki, S.; Matsunaga, N.; Nguyen, K. A.; Su, S. J.; Windus, T. L.; Dupuis, M.; Montgomery, J. A. *J. Comput. Chem.* **1993**, *14*, 1347.
(37) Pacios, L. F.; Christiansen, P. A. *J. Chem. Phys.* **1985**, *82*, 2664.
(38) Hurley, M. M.; Pacios, L. F.; Christiansen, P. A.; Ross, R.; Ermler, W. *J. Chem. Phys.* **1986**, *84*, 6840.
(39) Baybutt, L. R. K. P.; Truhlar, D. G. *J. Chem. Phys.* **1976**, *65*, 3826.
(40) Macchi, P.; Sironi, A. *Acta Crystallogr., Sect. A* **2004**, *60*, 502.

JP901753P